7.7; 11.4, 11.6; 14.7

Received 9 August 1971

Sound Attenuation in Lined Rectangular Ducts with Flow and Its Application to the Reduction of Aircraft Engine Noise

SUNG-HWAN KO

The Boeing Company, Seattle, Washington 98124

An investigation is made of the sound attenuation in a rectangular duct with two sides lined and with a uniform steady flow. It is found in the study of modal attenuation that the fundamental mode is not necessarily the least attenuated in lined ducts. It is shown that sound attenuation is influenced by the fluid flow; tuning frequency shifts to higher frequency with decreasing peak attenuation for downstream propagation and to lower frequency with increasing peak attenuation for upstream propagation. The effect of acoustic impedance on sound attenuation for a given duct geometry is presented as well as the effect of duct geometry on sound attenuation for a given acoustic impedance. Theoretically predicted attenuation spectra are compared with experimental results (test data for both rectangular flow duct and Boeing 747/JT9D engine). The predicted attenuation spectra are in very good agreement with the experimental results for downstream propagation. However, the present theory overpredicts the sound attenuation for upstream propagation.

INTRODUCTION

The objective of this study is to develop a theoretical method to predict the sound attenuation in acoustically lined ducts with flow, and to apply it to the problem of aircraft engine noise reduction. The reduction of fan noise and, in some cases, turbine noise, is important for today's aircraft. This turbomachinery noise can be effectively reduced by acoustically treating fan inlet and exhaust ducts.

The theoretical analysis is based on a rectangular duct with two sides lined in the presence of uniform flow. The present analysis provides the sound-attenuation spectrum for a given duct with specified acoustic lining parameters. Theoretically predicted attenuation spectra are compared with experimental results in order to determine the accuracy and validity of the present theory for its application to the reduction of aircraft noise.

Theoretical studies of the sound propagation in ducts have been made by many investigators: Morse,[1] Cremer,[2] Fischer and Andersson,[3] Rice,[4] Kurze,[5] and Doak and Vaidya[6] have studied the case of the duct without flow. Kurze has also presented experimental results for a duct with one side lined in the absence of flow. Benzakein, Kraft, and Smith[7] have presented a theoretical development, accompanied by an experimental check, of the attenuation in acoustically lined ducts with no flow. In order to investigate the effect of fluid flow on the sound attenuation, Meyer, Mechel, and Kurtze,[8] and Mechel, Mertens, and Schilze[9] conducted experimental work with a limited theoretical guidance. It is shown in their experiment that sound attenuation is influenced by Mach number. Extensive experimental measurements of sound attenuation in lined ducts with flow have been completed at Boeing, and the results have been reported by Haley.[10] In addition to these experimental investigations, Ingard[11] has shown theoretically the effect of Mach number on impedance, but no attempt has been made to obtain a complete analysis of sound attenuation. The effect of Mach number on the sound attenuation of the fundamental mode for rectangular ducts with one side lined has been investigated by Eversman.[12] Sound attenuation in an acoustically lined duct with a mean flow has been studied by Rice.[13]

None of these authors, however, has presented results similar to those obtained in the present work. In their investigations, some of the previous investigators studied the sound attenuation of the fundamental mode alone, assuming the fundamental mode is least attenuated. It is found in the study of the sound attenuation of each mode that the fundamental mode is not necessarily the least attenuated one in lined ducts. Multimodal eigenvalues are obtained and the sound-attenuation spectrum is calculated based on the acoustic energy flow, taking into account the effect of mean flow.

Pridmore-Brown,[14] Tack and Lambert,[15] Mungur and Gladwell,[16] Mungur and Plumblee,[17] Kurze and Allen,[18] and Mariano[19] studied the effect of boundary-layer refraction on the sound attenuation. These studies show that shear flow has influence on the sound attenuation, causing the attenuation to be lower for upstream propagation (the case where flow is in the opposite direction of wave propagation) and higher for downstream propagation (the case where flow is in the direction of wave propagation).

I. ANALYTICAL MODEL

A. General

The analytical model considered in the present study is a rectangular duct with two sides lined in the presence of a uniform fluid flow. Geometry of an acoustically lined duct is shown in Fig. 1. The fluid flow is assumed to be in the z direction and to be uniform on the cross section of the duct. The walls of the duct perpendicular to the x axis are treated with acoustic lining material, while the other two walls are not lined. The acoustic lining is a porous sheet (fibrous metal or perforated sheet) mounted on a locally reacting core with impervious backing (see Fig. 2). The depth of the material is known as lining thickness or core depth. The lining impedance (soft-wall boundary condition) is assumed to be uniform through the duct.

The propagation of sound in a duct with a uniform flow is described by the wave equation, the solution of which is the velocity potential of the small disturbance:

$$\frac{1}{c^2}\left(\frac{\partial}{\partial t}+w_0\frac{\partial}{\partial z}\right)^2\psi=\left(\frac{\partial^2}{\partial x^2}+\frac{\partial^2}{\partial y^2}+\frac{\partial^2}{\partial z^2}\right)\psi, \qquad (1)$$

where ψ is the velocity disturbance potential defined by $\mathbf{v}=-\nabla\psi$; $\mathbf{v}$ is the velocity disturbance vector; c is the speed of sound; w_0 is uniform velocity in the z direction; t is time; and x, y, and z are spatial coordinates, assuming that no effect of viscosity and no heat transfer are present.

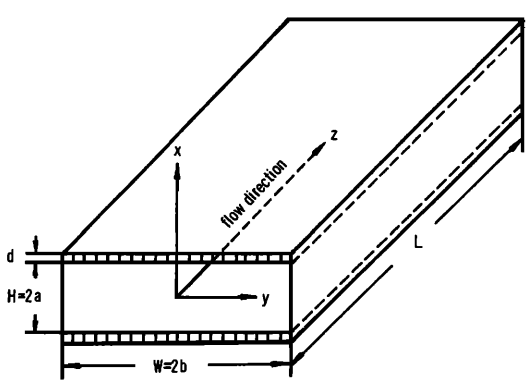

FIG. 1. Geometry of an acoustically lined rectangular duct.

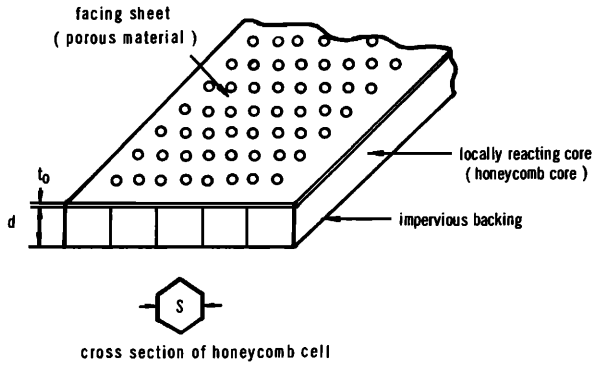

FIG. 2. Configuration of acoustic lining.

B. Eigenvalue Equations

The velocity disturbance potential is, for sound-wave propagation, written as

$$\psi=\varphi(x,y)e^{-i(k_{mn}z-\omega t)}, \qquad (2)$$

where $\varphi(x,y)$ is the complex amplitude, ω is the angular frequency of sound wave, and k_{mn} is the wave constant whose imaginary part represents the rate of decay along the z direction; $\mathrm{Im}(k_{mn})<0$ for downstream wave propagation, $\mathrm{Im}(k_{mn})>0$ for upstream wave propagation, and $\mathrm{Re}(k_{mn})>0$ for both cases.

By the method of separation of variables, the solution of Eq. 1 can be written as:

$$\psi_{mn}=(A_me^{ik_mx}+B_me^{-ik_mx})\times(C_ne^{ik_ny}+D_ne^{-ik_ny})e^{-i(k_{mn}z-\omega t)}, \qquad (3)$$

where k_m and k_n are wave constants, and A_m, B_m, C_n, and D_n are arbitrary constants which can be determined from pertinent boundary conditions. It should be noted that both symmetrical and antisymmetrical modes exist on the cross section (x–y plane) of the duct in both the x and y directions. In the y direction, $\partial\psi(x,0)/\partial y=0$ for symmetrical modes, and $\psi(x,0)=0$ for antisymmetrical modes. In the x direction, $\partial\psi(0,y)/\partial x=0$ for symmetrical modes, and $\psi(0,y)=0$ for antisymmetrical modes.

If the above boundary conditions are used, then solutions of the wave equation are written as follows:

$$\psi_{mn}=4A_mC_n\cos k_mx\begin{Bmatrix}\cos k_ny\\ i\sin k_ny\end{Bmatrix}e^{-i(k_{mn}z-\omega t)} \qquad (4)$$

for symmetrical modes in the x direction, and

$$\psi_{mn}=4A_mC_ni\sin k_mx\begin{Bmatrix}\cos k_ny\\ i\sin k_ny\end{Bmatrix}e^{-i(k_{mn}z-\omega t)} \qquad (5)$$

for antisymmetrical modes in the x direction, where $\cos k_ny$ and $\sin k_ny$ are symmetrical and antisymmetrical modes in the y direction.

Substituting Eqs. 4 or 5 into Eq. 1 yields

$$k_{mn}=\frac{-kM+[k^2-(1-M^2)(k_m^2+k_n^2)]^{\frac{1}{2}}}{(1-M^2)}, \quad (6)$$

where $k=\omega/c$ is the wavenumber and $M=w_0/c$ is the Mach number of mean flow in a duct.

Solutions of k_m and k_n can be obtained from wall boundary conditions. It should be noted that the normal component of the velocity disturbance vanishes at the rigid wall (unlined wall or hard wall), while this is finite at the soft wall (lined wall or treated wall).

The boundary condition at the rigid wall is given by

$$(\partial\psi/\partial y)_{y=\pm b}=0, \quad (7)$$

where $2b$ is duct width, and the condition Eq. 7 yields

$$k_n=n\pi/2b \quad (n=0, 1, 2, 3, \cdots). \quad (8)$$

The boundary condition at the soft wall is given by

$$(\partial\psi/\partial x)_{x=\pm a}\neq 0, \quad (9)$$

where $2a$ is duct height.

The development of the eigenvalue equation is conceptually based on the investigation of the stability of a plane vortex sheet (see, e.g., Miles[20] and Lessen, Fox, and Zien[21] among many investigators). In their study of the stability of the inviscid jets in compressible fluid, Lesson, Fox, and Zien used the pressure matching condition at the outer and inner sides of the vortex sheet. In the present analysis, the boundary condition to be satisfied on the soft wall (acoustic lining) is interpreted as the boundary between two media separated by a plane vortex sheet, the displacement of which is written as

$$\zeta'=\zeta e^{-i(k_{mn}z-\omega t)}, \quad (10)$$

where ζ is the amplitude of the vortex sheet displacement ζ'. It is noted in the present analysis that the displacement of the vortex sheet is equal to the particle displacement in the acoustic lining. The rate of change of the displacement of the particle in the lining (the side of the vortex sheet where the fluid axial velocity is zero) is equal to the normal component of the velocity disturbance. At the outer surface of the vortex sheet, the amplitude of the velocity disturbance u' in the x direction is written as

$$u_m=i\zeta_m(\omega-k_{mn}w_0), \quad (11)$$

where u_m is the amplitude of the velocity disturbance u', and ζ_m is the amplitude of the particle displacement ζ' at the outer surface of the vortex sheet (free-stream side).

If the velocity and pressure disturbances are substituted into the linearized momentum equation (in the x direction)

$$\rho\left(\frac{\partial u'}{\partial t}+w_0\frac{\partial u'}{\partial z}\right)=-\frac{\partial p'}{\partial x}, \quad (12)$$

then Eq. 12 becomes

$$i\rho u_m(\omega-k_{mn}w_0)=-(\partial p_m/\partial x) \quad (13)$$

at the outer surface of the vortex sheet, where ρ is the density of fluid, and u_m and p_m are the amplitudes of the velocity and pressure disturbances (u' and p'), respectively.

Since the rate of change of the displacement of the vortex sheet equals the velocity disturbance at the sheet, the normal component of the velocity disturbance at the inner surface of the vortex sheet can be written as

$$u_w=i\omega\zeta_w, \quad (14)$$

where u_w is the amplitude of the velocity disturbance and ζ_w is the amplitude of the particle displacement in the x direction at the inner surface of the vortex sheet.

Define the specific admittance ratio at $x=-a$ as

$$Y=-\rho c(u_w/p_w), \quad (15)$$

where Y is the specific admittance ratio and p_w is the amplitude of the pressure disturbance at the inner surface.

With the pressure and displacement matching conditions on both sides of the vortex sheet, combining Eqs. 11, 13, 14, and 15 yields

$$-\frac{Y}{i\omega c}p'=\frac{\partial p'/\partial x}{(\omega-k_{mn}w_0)^2}. \quad (16)$$

Combining Eq. 2 and the linearized momentum equation (in the z direction), and integrating the resulting expression over z gives

$$p'=i\rho(\omega-k_{mn}w_0)\psi. \quad (17)$$

Combining Eqs. 16 and 17 gives

$$ikY\left(1-\frac{k_{mn}}{k}M\right)^2=\frac{\partial\psi/\partial x}{\psi}. \quad (18)$$

If Eqs. 4 and 5 are substituted into Eq. 18, then a set of eigenvalue equations can be written as

$$iakY\left(1-\frac{k_{mn}}{k}M\right)^2=ak_m\tan(ak_m) \quad (19)$$

for symmetrical modes in the x direction, and

$$iakY\left(1-\frac{k_{mn}}{k}M\right)^2=-ak_m\cot(ak_m) \quad (20)$$

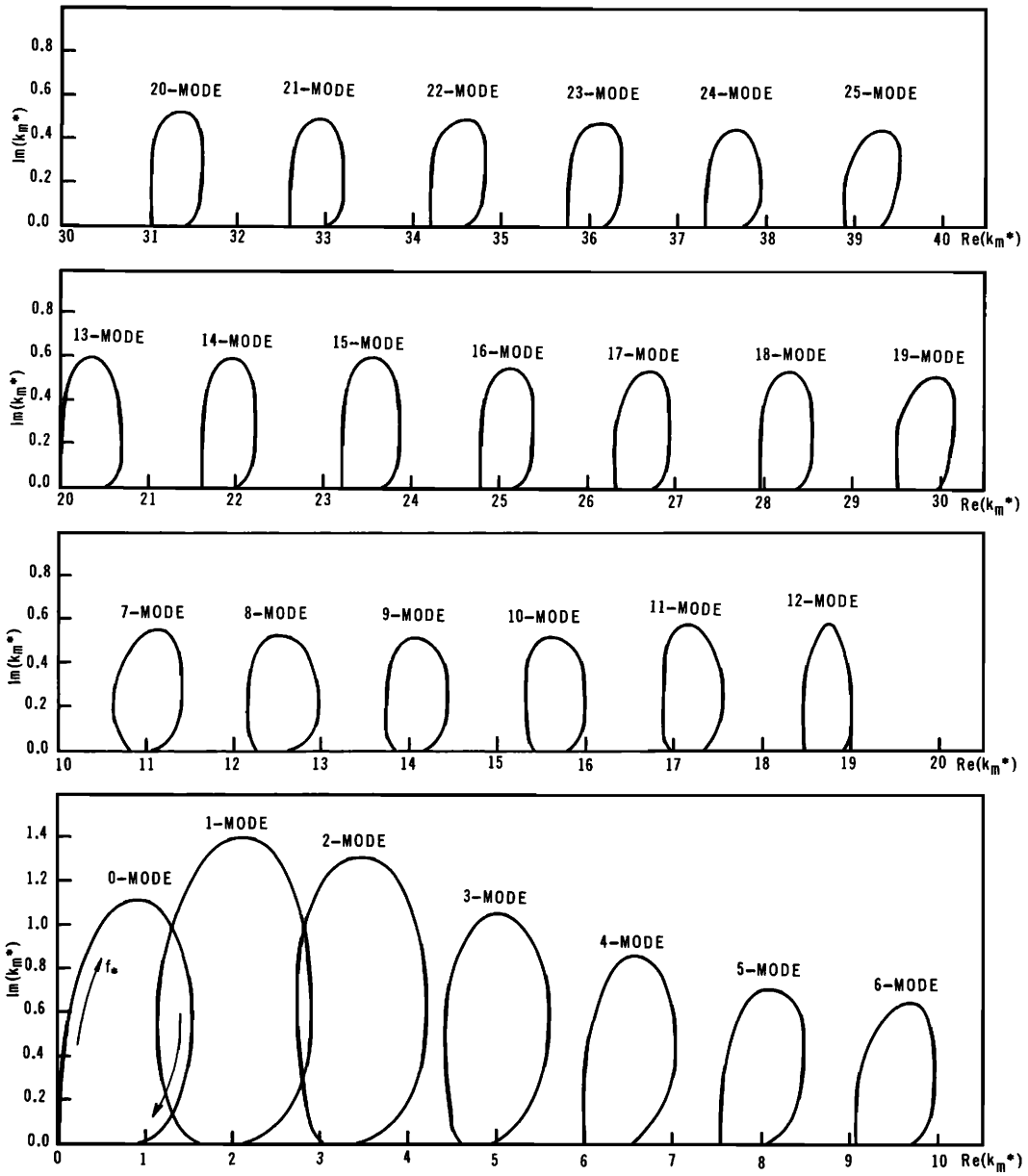

FIG. 3. Solution of eigenvalue k_m^* for given parametric values; $M=0.36$, $R_*=2.0$, $f_0^*=17.92$, and $d_*=0.03374$ for the range of $f_*=0$ to 15 (clockwise direction).

for antisymmetrical modes in the x direction. The eigenvalues k_m and k_{mn} can be obtained from solutions of Eqs. 19 and 20 for a given duct geometry, Mach number, and specific acoustic admittance ratio.

C. Description of Soft-Wall Boundary Condition

In the present study, the soft-wall boundary condition is described by an impedance model. Acoustic impedance of a single-layer lining is composed of (1) facing-sheet impedance (resistance and reactance) and (2) air-cavity impedance. Air-cavity impedance is the contribution of the sound wave reflected from the rigid wall and is equivalent to the input impedance of a tube whose end is closed by a rigid cap.

The present acoustic lining impedance is given by

$$z_*=R_*\left(1+i\frac{f}{f_0}\right)-i\cot(kd), \tag{21}$$

where $z_*=z/\rho c$ is the specific acoustic impedance ratio, z is the specific acoustic impedance (cgs rayls), ρc is the characteristic impedance of air (cgs rayls; e.g., $\rho c=41.6$ rayls at standard conditions), $R_*=R/\rho c$ is the specific acoustic resistance ratio or nondimensional

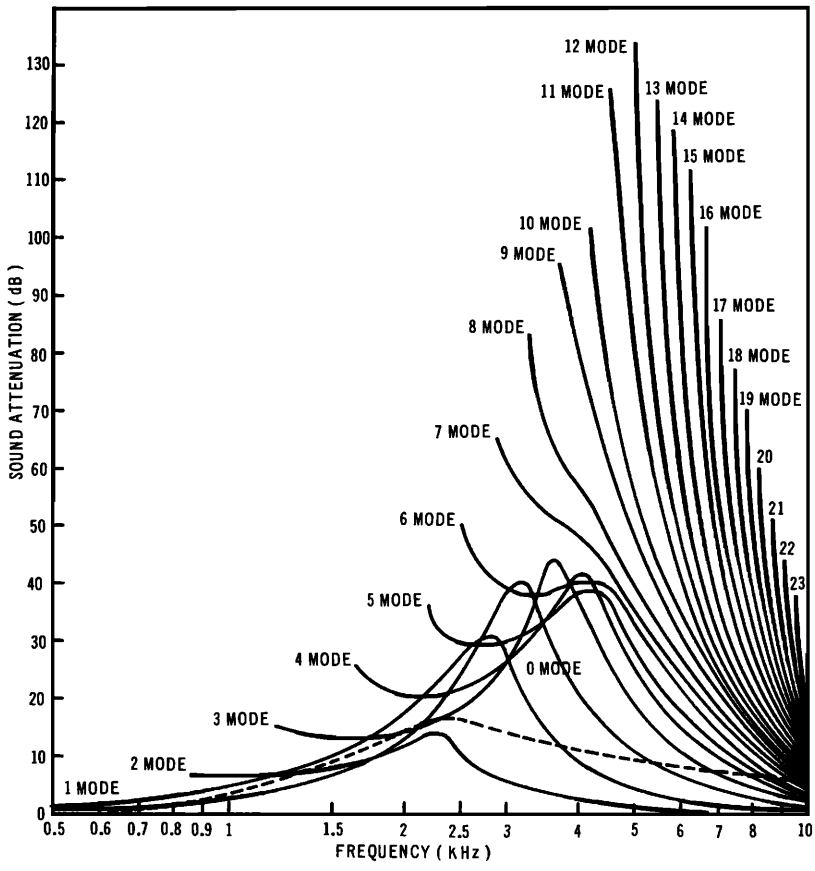

FIG. 4. Sound-attenuation spectra of each mode (above cutoff frequency) for the given duct height $H=16.3$ in. with parametric values: $M=0.36$, $R_*=1.5$, $f_0=15\,000$ Hz, $d=0.55$ in., $L=59$ in., and $c=1137$ ft/sec; (——): modal attenuation; (– – –): total attenuation.

flow resistance, f is the frequency (in hertz) of the sound wave, f_0 is the characteristic frequency (in hertz) of facing sheet, k is wavenumber (in in.$^{-1}$), and d is lining depth in inches. The specific acoustic admittance ratio Y is the reciprocal of z_*. The first term, $R_*(1+if/f_0)$, of Eq. 21 represents the impedance of the facing sheet, and air-cavity impedance is represented by the second term, $-i\cot(kd)$, of Eq. 21.

D. Solution of Eigenvalues

The determination of eigenvalues k_m and k_{mn} for each mode was a major problem solved in the present study. Eigenvalues k_m and k_{mn} can be obtained by solutions of Eqs. 19 and 20 for given physical parameters. In order to minimize the number of physical parameters, the following nondimensional quantities are introduced:

$M=w_0/c$, Mach number;
$f_*=fH/c$, nondimensional frequency parameter;
$R_*=R/\rho c$, nondimensional flow resistance;
$f_{0*}=f_0H/c$, nondimensional characteristic frequency;
$d_*=d/H$, nondimensional cavity depth;
$L_*=L/H$, nondimensional duct length.

Accordingly, nondimensional eigenvalue equations can be written as

$$i\pi f_* Y\left(1-\frac{k_{mn}^*}{k^*}M\right)^2=k_m^*\tan k_m^*, \tag{22}$$

$$i\pi f_* Y\left(1-\frac{k_{mn}^*}{k^*}M\right)^2=-k_m^*\cot k_m^*, \tag{23}$$

$$\frac{k_{mn}^*}{k_*}=\frac{-M+\{1-(1-M^2)[(k_m^*/k_*)^2+(k_n^*/k_*)^2]\}^{\frac{1}{2}}}{(1-M^2)}, \tag{24}$$

where $k_m^*=ak_m$, $k_n^*=ak_n$, and $k_{mn}^*=ak_{mn}$ are nondimensional eigenvalues, and $k_*=ak=\pi f_*$ is the nondimensional wavenumber.

In the present investigation, Eqs. 22 and 23 were numerically solved for assigned values of M, f_*, R_*, f_0^*, and d_*. The computational procedure was first to find eigenvalues k_m^* for the case of a nearly rigid wall, and to use these values of k_m^* as initial values. Then, by means of the Newton–Ralphson method, the eigenvalues k_m^* were successively approximated until no virtual changes in the sixth decimal place of $|k_m^*|$ were forthcoming for a range of f_* with assigned values

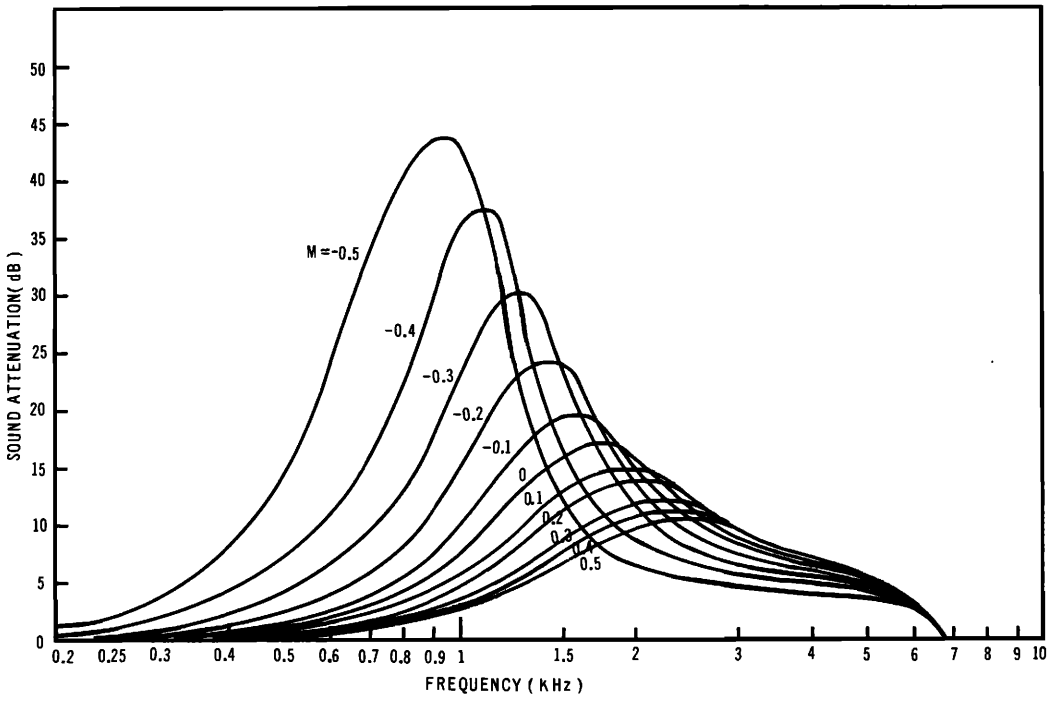

FIG. 5. Effect of mean Mach number of air flow on the sound attenuation for given parametric values: $R_*=1.5$, $f_0=15\,000$ Hz, $d=1$ in., $H=7.375$ in., $L=16$ in., and $c=1120$ ft/sec.

of M, R_*, $f_0{}^*$, and d_*. An example of the solutions of Eqs. 22 and 23 is shown in Fig. 3. All calculations reported in the present work were performed on a CDC 6600 computer at Boeing.

E. Acoustic Energy Attenuation

Blokhintsev[22] has derived the mean flow energy density and the mean energy flow for acoustic wave propagation in a medium at rest. On the basis of his derivation, Eversman[23] has obtained the mean acoustic energy flow in a hard-wall duct with uniform steady flow. In a method similar to that employed by him, the expression of acoustic energy transmission in a lined duct with uniform flow has been obtained by Ko[24] as shown below.

For the mn mode, the acoustic energy flow can be written as

$$E_{mn}(z)=|C_0|^2\rho c(abk^2)\frac{\sinh(2a\beta_m)}{2a\beta_m}$$
$$\times\left\{M\left[1+\left|\frac{k_m}{k}\right|^2+\left(\frac{k_n}{k}\right)^2-(1-M^2)\left|\frac{k_{mn}}{k}\right|^2\right]+(1-M^2)\frac{2\alpha_{mn}}{k}\right\}e^{2\beta_{mn}z}, \quad (25)$$

where C_0 is a constant, $k_m=\alpha_m+i\beta_m$, and $k_{mn}=\alpha_{mn}+i\beta_{mn}$. Sound attenuation in a lined duct is defined as a decrease in sound energy (in decibels) measured at the same point in space before and after an acoustic lining material is inserted between noise source and measurement point. Therefore, the sound attenuation due to an acoustic lining is equal to the decrease in the acoustic energy flows (in decibels) computed at the entrance and the exit of the lined duct.

The total sound attenuation in a lined duct is written as

$$\Delta PWL=10\log_{10}\sum_m\sum_n E_{mn}(0)/\sum_m\sum_n E_{mn}(L), \quad (26)$$

where ΔPWL is the sound attenuation which represents the decrease of the acoustic energy flow expressed in decibels, and $E_{mn}(0)$ and $E_{mn}(L)$ are acoustic energy flows at the entrance and the exit of the duct, respectively.

II. THEORETICAL RESULTS

A. Modal Attenuation

A study of sound attenuation in a lined duct for each mode was conducted in order to find the least attenuated mode. Previous studies by many investigators have indicated that the fundamental mode (denoted the 0-mode in this work) is the least attenuated one. However, the result of the present study shows in Fig. 4 that the fundamental mode is not necessarily the least attenuated one in a lined duct.

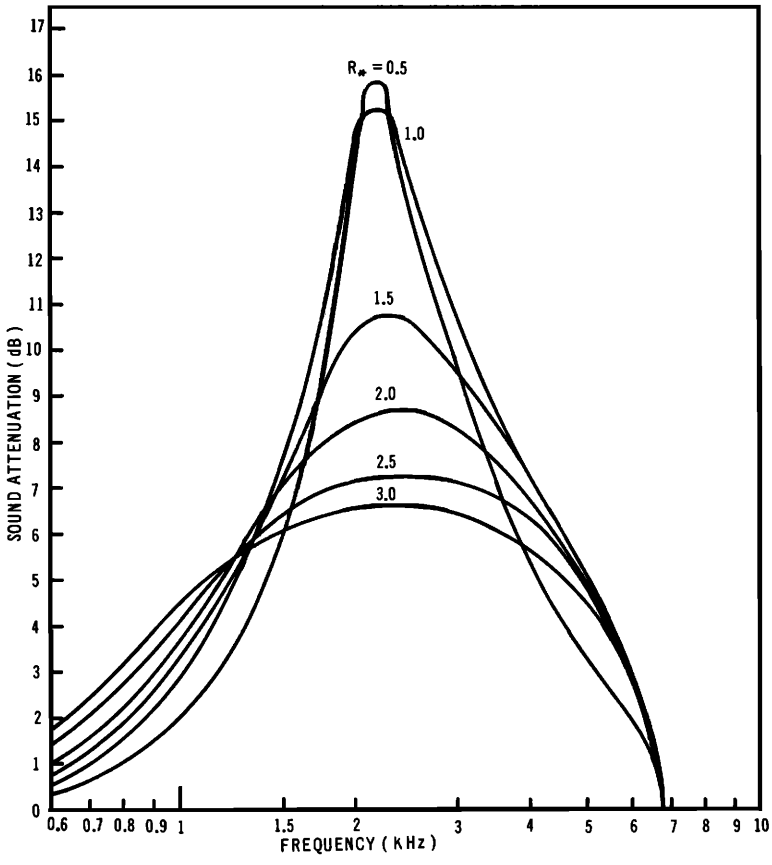

FIG. 6. Effect of acoustic resistance on the sound attenuation for given parametric values: $M=0.4$, $f_0=15\,000$ Hz, $d=1$ in., $H=7.375$ in., $L=16$ in., and $c=1120$ ft/sec.

Attenuation spectra for each mode above hard-wall cutoff frequency are shown in Fig. 4. In the calculation of sound attenuation for the given parameters, 24 modes were required to obtain the complete sound attenuation spectrum over a frequency range of 0 to 10 000 Hz. It is important to note that total sound attenuation is strongly dependent on the least attenuated mode. In the present investigation, the two-dimensional wave equation was considered, i.e., $kb \ll 1$.

B. Effects of Physical Parameters on Sound Attenuation

A number of parametric studies were conducted in order to find the effects of various physical parameters on sound attenuation in a lined duct. The two-dimensional wave equation was used in this section; i.e., $kb \ll 1$. Experimental results of parametric studies of the acoustic behavior of duct-lining materials are presented in Ref. 25, and their trends of the acoustic behavior in lined ducts agree with the present work. The results presented in this section are for specific values of other parameters and thus should not be regarded as general.

1. Effect of Mach Number on Sound Attenuation

The effect of Mach number on sound attenuation was made for assigned values of R_*, f_0, d, H, L, and c. As can be seen in Fig. 5, tuning frequency (frequency of peak attenuation) shifts to higher frequency with decreasing peak attenuation for downstream propagation and to lower frequency with increasing peak attenuation for upstream propagation.

2. Effect of Nondimensional Flow Resistance on Sound Attenuation

The effect of nondimensional flow resistance on sound attenuation is presented in Fig. 6. As is shown in the figure, the level of peak attenuation decreases with broadening bandwidth, keeping tuning frequency approximately constant as the value of R_* increases for assigned values of M, f_0, d, H, L, and c. Acoustic lining material (facing sheet) having lower values of R_* may be adequate for reducing a pure tone, whereas a facing sheet with higher values of R_* may be more suitable for reducing a series of pure tones or broadband noise. Although lower flow resistance provides higher peak attenuation, this trend may not be considered as general.

3. Effect of Characteristic Frequency of Lining Material on Sound Attenuation

Figure 7 shows the effect of the characteristic frequency of facing sheet on sound attenuation. It was

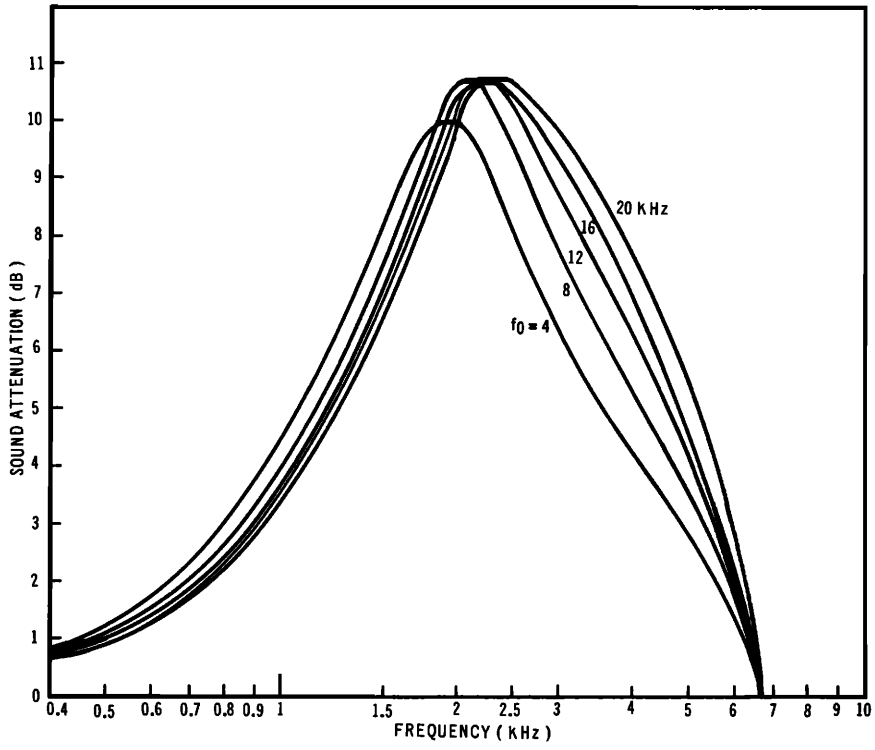

FIG. 7. Effect of characteristic frequency of acoustic lining material on the sound attenuation for given parametric values: $M=0.4$, $R_*=1.5$, $d=1$ in., $H=7.375$ in., $L=16$ in., and $c=1120$ ft/sec.

found that in the present case no substantial changes in sound attenuation spectra occurred for the values of f_0 above 20 000 Hz for assigned values of M, R_*, d, H, L, and c. In general, as the value of f_0 increases, tuning frequency shifts to higher frequency with broadening bandwidth.

4. Effect of Acoustic Lining Depth on Sound Attenuation

Figure 8 shows the effect of lining depth on sound attenuation. The frequency of peak attenuation shifts to higher frequency with a moderate change in the level of peak attenuation, as lining thickness decreases.

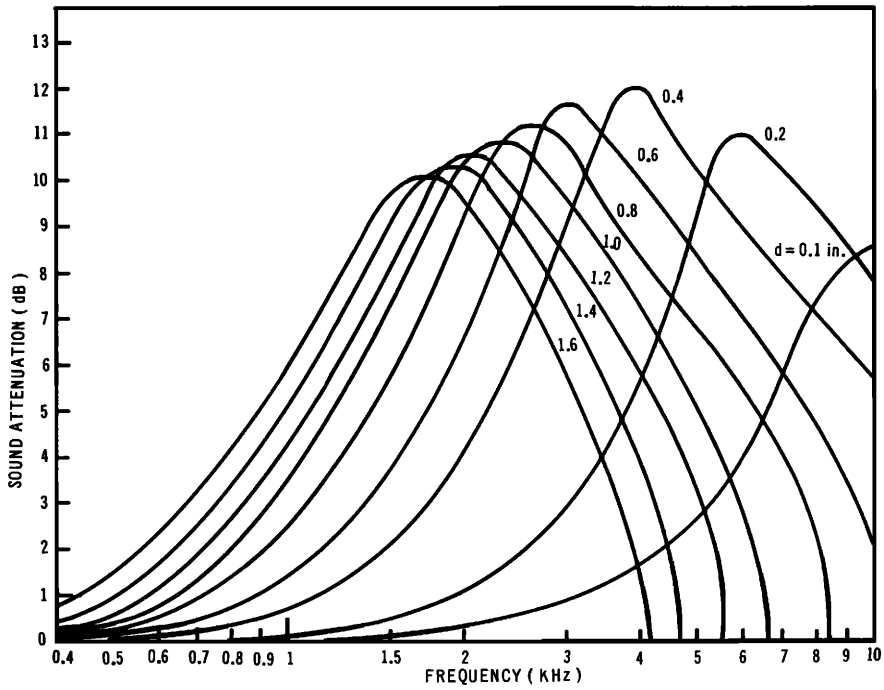

FIG. 8. Effect of acoustic lining depth on the sound attenuation for given parametric values: $M=0.4$, $R_*=1.5$, $f_0=15\,000$ Hz, $H=7.375$ in., $L=16$ in., and $c=1120$ ft/sec.

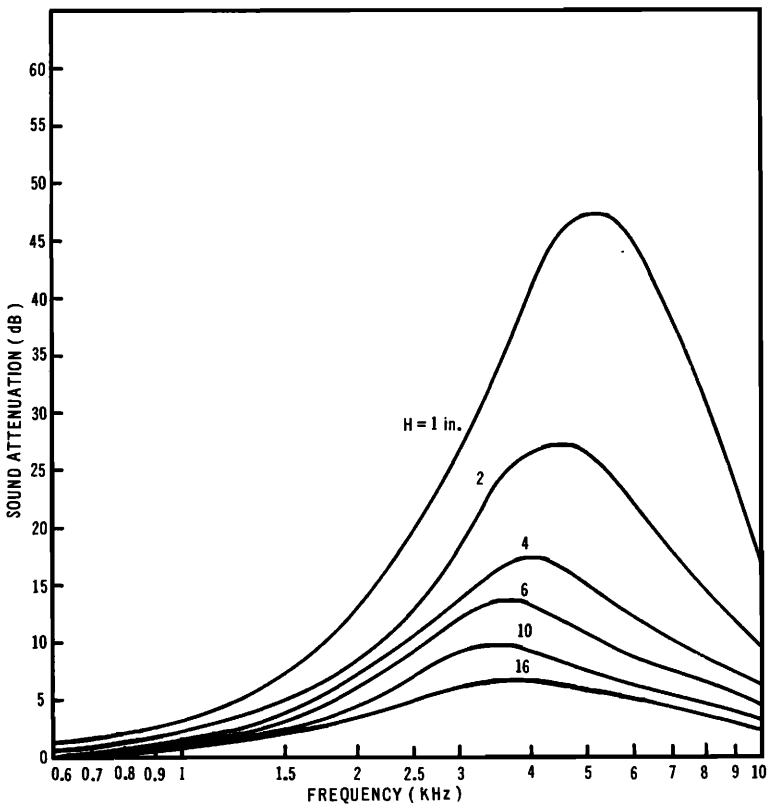

FIG. 9. Effect of duct height on the sound attenuation for given parametric values: $M=0.4$, $R_*=1.5$, $f_0=15\,000$ Hz, $d=0.5$ in., $L=16$ in., and $c=1120$ ft/sec.

In Fig. 8, maximum peak attenuation is 12 dB at the tuning frequency of 3900 Hz, with an optimum lining depth of $d=0.4$ in. for assigned values of M, R_*, f_0, H, L, and c.

5. Effect of Duct Geometry on Sound Attenuation

The effects of duct height and length on sound attenuation are shown in Figs. 9 and 10, respectively. It is shown in Fig. 9 that the level of sound attenuation becomes higher with higher values of tuning frequency as duct height decreases for assigned values of M, R_*, f_0, d, L, and c. It is shown in Fig. 10 that the level of sound attenuation becomes higher with lower values of tuning frequency as duct length increases for assigned values of M, R_*, f_0, d, H, and c. A rigorous study requires examining the nondimensional parameters of f_* and L_* for given values of M, R_* f_{0*}, and d_*.

III. COMPARISON OF THEORY AND EXPERIMENT

A. Flow Duct

Comparisons of theoretically predicted sound-attenuation spectra and lining attenuation test data are presented in Figs. 11–15 for a rectangular flow duct (Ref. 10). Theoretically predicted attenuation spectra are in very good agreement with test data for downstream propagation and in poor agreement with test data for upstream propagation. This is probably due to the effect of refraction of the sound waves by the shear layer; the wavefront is refracted away from the boundary (acoustic lining) for upstream propagation in the presence of flow. This yields a less normal angle of incidence than in the absence of flow, causing less attenuation. It is noted in Figs. 11 and 12 that the discrepancy between theoretical and experimental results occurs at low frequencies and becomes greater as Mach number increases for upstream propagation. The phenomenon for downstream propagation is opposite to that of upstream propagation. However, the present theory indicates that the effect of refraction by a boundary layer is more influential for upstream propagation than for downstream propagation (based on the comparisons of theoretical and experimental results).

It is also important to mention that nondimensional flow resistance is affected by bonding of lining materials, by grazing flow, by operating over-all sound-pressure level, and by static temperature and pressure in the duct. Correction of these effects was properly taken into account for each Mach number on the basis of experimentally determined correction values.

The acoustic lining material (facing sheet) used in the flow duct test was fibrous material mounted on honeycomb core. The characteristic frequency of the facing sheet was assumed to be $f_0=15\,000$ Hz.

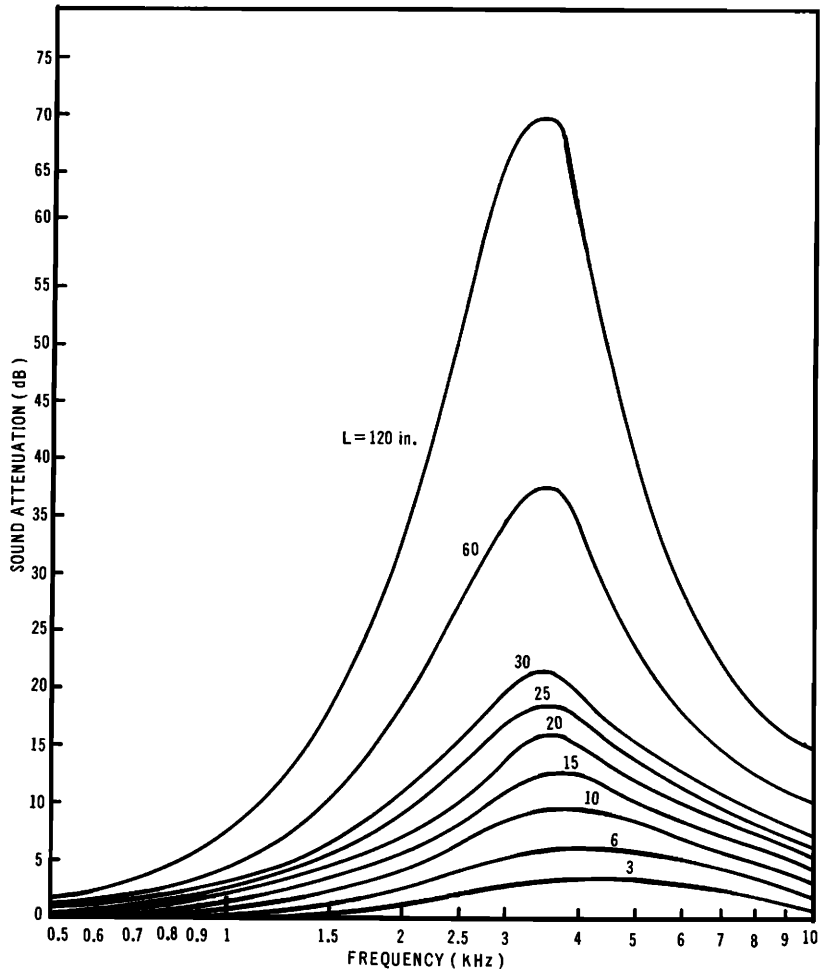

FIG. 10. Effect of duct length on the sound attenuation for given parametric values: $M=0.4$, $R_*=1.5$, $f_0=15\,000$ Hz, $d=0.5$ in., $H=6$ in., and $c=1120$ ft/sec.

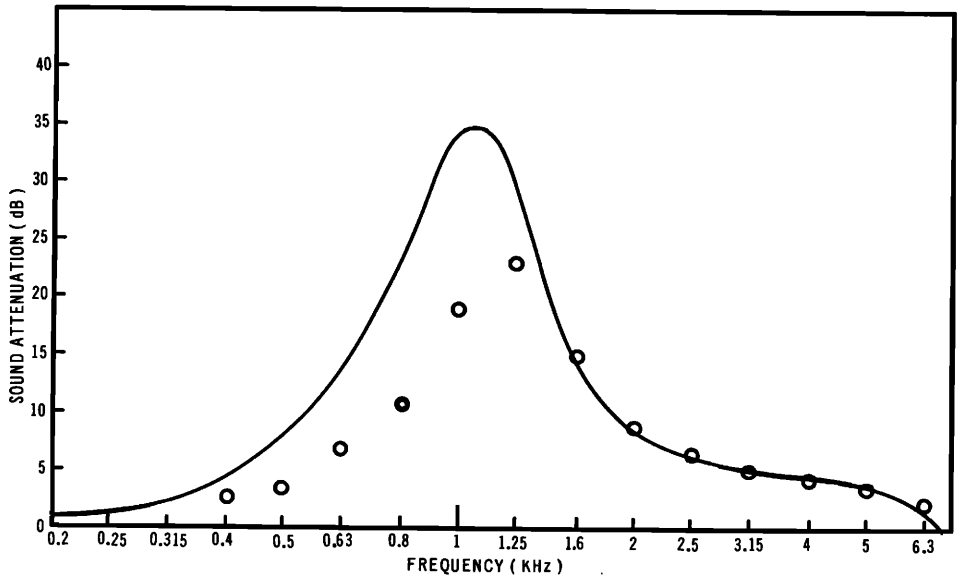

FIG. 11. Comparison of the theoretical and experimental results for given parametric values: $M=-0.4$, $R_*=1.61$, $f_0=15\,000$ Hz, $d=1$ in., $H=7.375$ in., $L=16$ in., $W=12$ in., and $c=1089$ ft/sec; (——): theory; ○: test data.

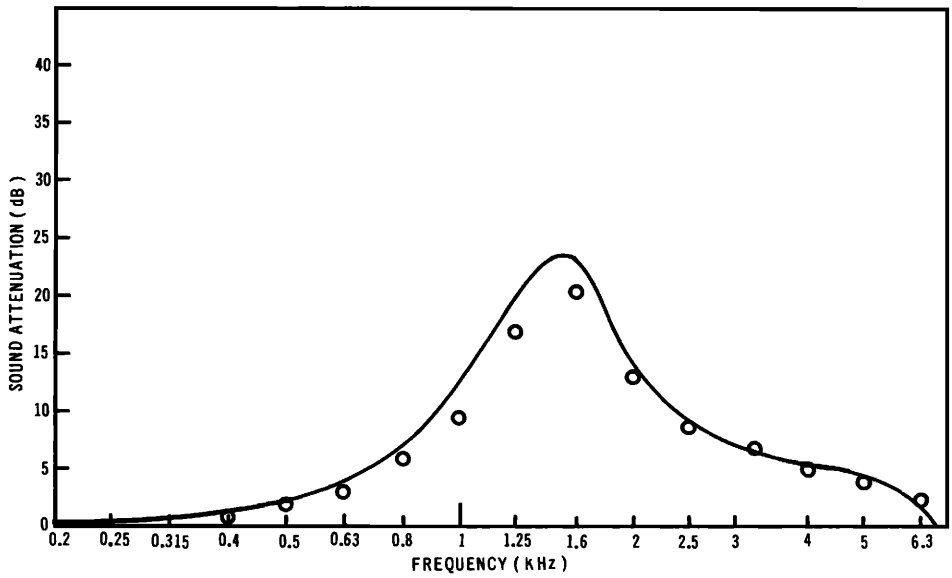

FIG. 12. Comparison of the theoretical and experimental results for given parametric values; $M=-0.15$, $R_*=1.43$, $f_0=15\,000$ Hz, $d=1$ in., $H=7.375$ in., $L=16$ in., $W=12$ in., and $c=1107$ ft/sec; (——): theory; ○: test data.

B. Real Engine (Boeing 747/JT9D Engine)

An analysis of sound attenuation in a rectangular duct with two sides lined with flow has been applied to the computation of sound attenuation in an annular JT9D fan exhaust duct with two sides lined. In treating the actual engine ducts, all of the apparently available areas cannot be acoustically treated because of the bifurcations, acoustic panel installation joints, radial struts, etc. Therefore, the areas unavailable for acoustic treatment must be accounted for in calculating the sound attenuation. In order to account for the effect of treated area loss for sound attenuation in a duct with two sides lined, geometric and effective duct lengths are introduced as follows:

Nondimensional geometric duct length is defined by

$$\left(\frac{L}{H}\right)=\frac{1}{2}\frac{\text{treated area with no area loss}}{\text{flow area}} \tag{27}$$

and nondimensional effective duct length is defined by

$$\left(\frac{L}{H}\right)_e=\frac{1}{2}\frac{\text{treated area observing area loss}}{\text{flow area}}\leq\left(\frac{L}{H}\right). \tag{28}$$

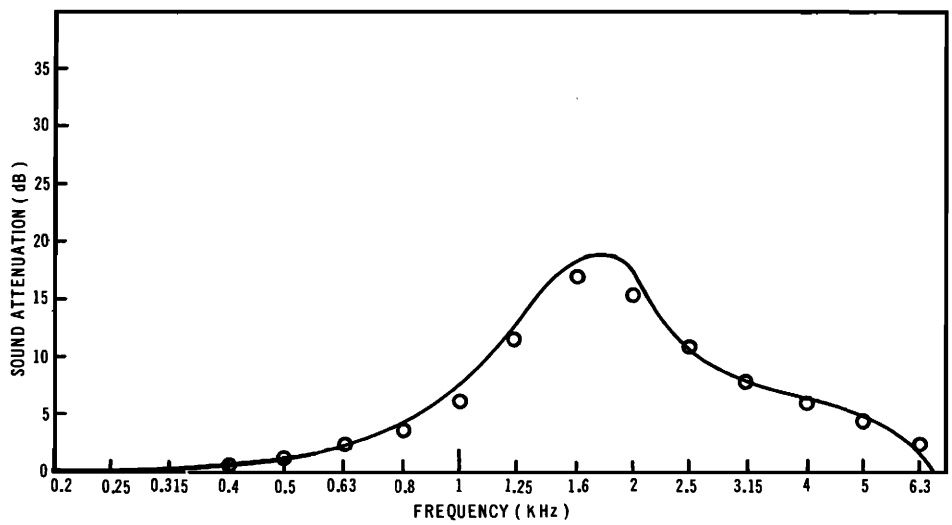

FIG. 13. Comparison of the theoretical and experimental results for given parametric values: $M=0$, $R_*=1.40$, $f_0=15\,000$ Hz, $d=1$ in., $H=7.375$ in., $L=16$ in., $W=12$ in., and $c=1132.2$ ft/sec; (——): theory; ○: test data.

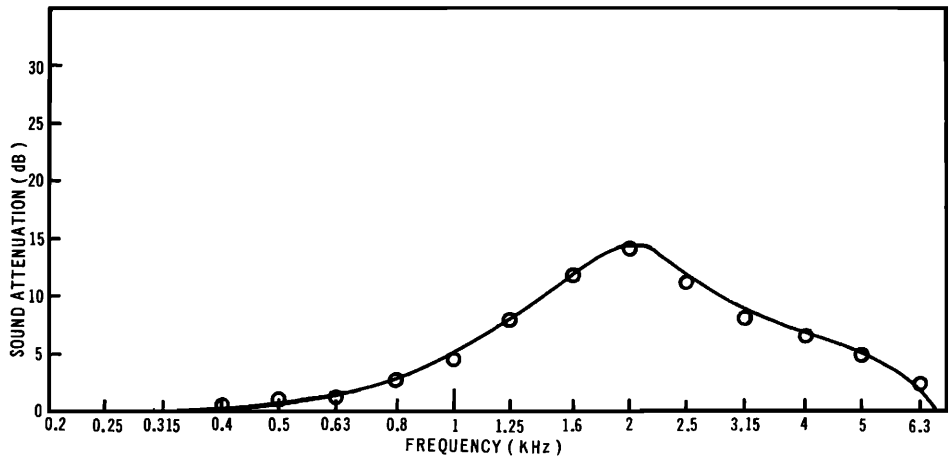

FIG. 14. Comparison of the theoretical and experimental results for given parametric values: $M=0.2$, $R_*=1.40$, $f_0=15\,000$ Hz, $d=1$ in., $H=7.375$ in., $L=16$ in., $W=12$ in., and $c=1131.1$ ft/sec; (——): theory; ○: test data.

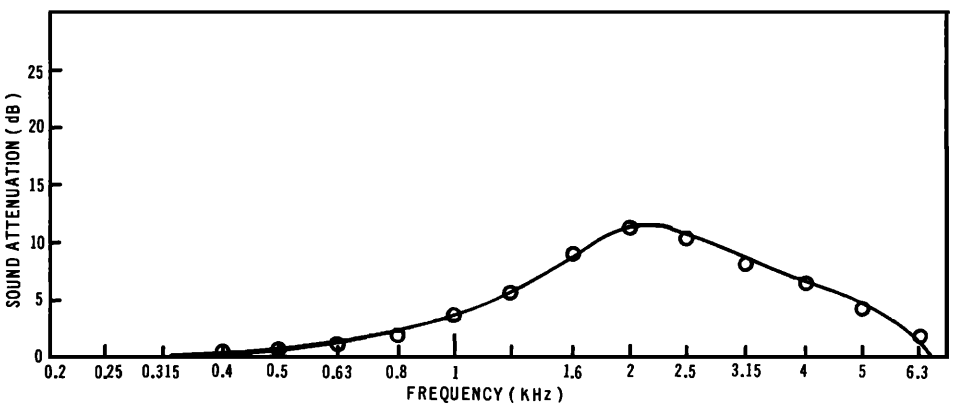

FIG. 15. Comparison of the theoretical and experimental results for given parametric values: $M=0.4$, $R_*=1.51$, $f_0=15\,000$ Hz, $d=1$ in., $H=7.375$ in., $L=16$ in., $W=12$ in., and $c=1100$ ft/sec; (——): theory; ○: test data.

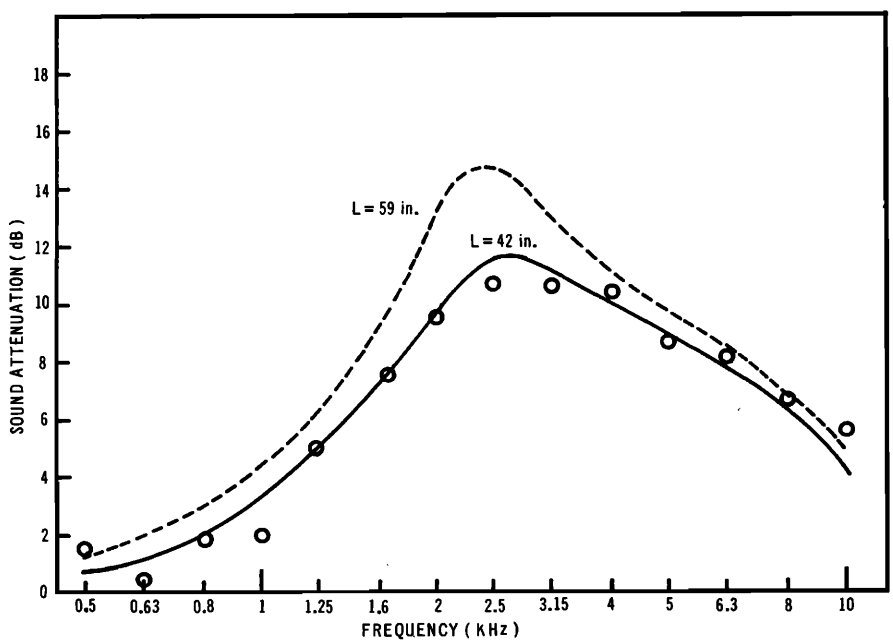

FIG. 16. Comparison of the theoretical result and test data for Boeing 747/JT9D engine exhaust duct: $M=0.36$, $R_*=2.0$, $f_0=15\,000$ Hz, $d=0.55$ in., $H=16.3$ in., and $c=1137$ ft/sec; (——): theoretical result based on effective duct length; (– – –): theoretical result based on geometric duct length; ○: full-scale engine test data ($\frac{1}{3}$-oct bandwidth) measured at 115° from duct inlet.

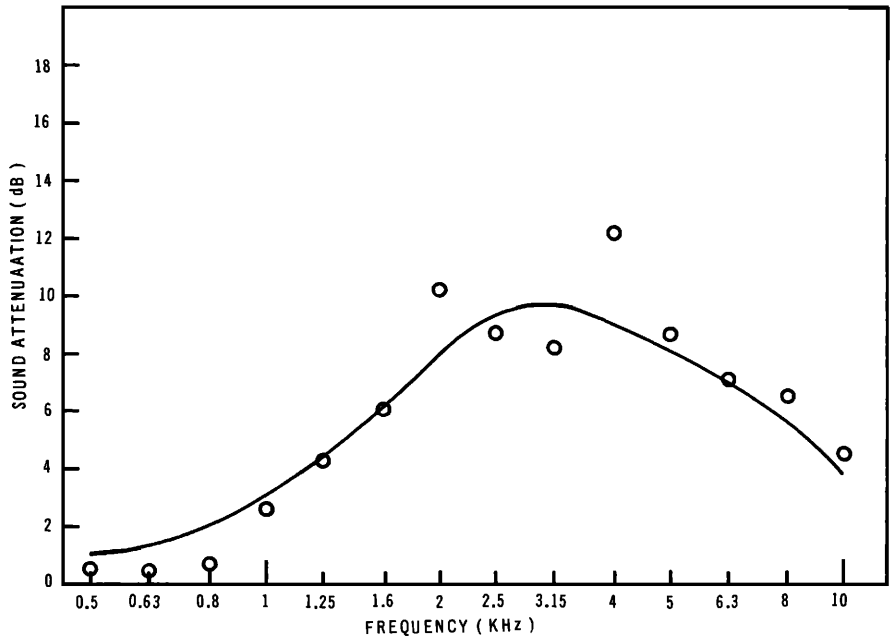

FIG. 17. Comparison of the theoretical result and test data for Boeing 747/JT9D engine exhaust duct: $M=0.43$, $R_s=2.5$, $f_0=15\,000$ Hz, $d=0.55$ in., $H=16.3$ in., $L=42$ in., and $c=1148$ ft/sec; (——): theoretical result based on effective duct length; ○: full-scale engine test data ($\frac{1}{3}$-oct bandwidth) measured at 115° from duct inlet.

Sound attenuation is the difference between sound-pressure levels (in decibels) for the hard-wall and treated cases measured at the same microphone locations for the same engine operating condition. In the present testing, microphones were located at polar angles (5° or 10° apart) with a 200-ft radius from the central position of the engine. Acoustic test data were based on the $\frac{1}{3}$-oct band analysis from 50 to 10 000 Hz. The acoustic lining used in the present testing was Rigimesh (a fibrous woven material having the characteristic frequency $f_0=15\,000$ Hz) facing sheet bonded on honeycomb core. In Fig. 16, theoretically predicted sound attenuation based on effective duct length (or actual treated area) is compared with that of geometric duct length (or available area), and these two are compared with full-scale engine test data measured at the angle of maximum attenuation (115° from engine inlet). As can be seen in the figure, the theoretical result based on the effective duct length is in better agreement with the test data than that based

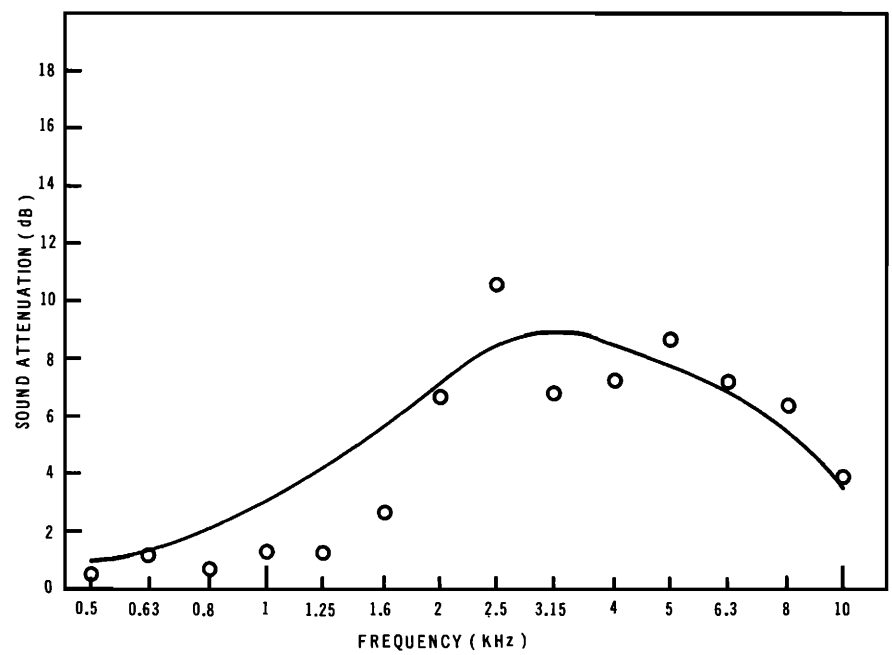

FIG. 18. Comparison of the theoretical result and test data for Boeing 747/JT9D engine exhaust duct: $M=0.47$, $R_s=2.7$, $f_0=15\,000$ Hz, $d=0.55$ in., $H=16.3$ in., $L=42$ in., and $c=1160$ ft/sec; (——): theoretical result based on effective duct length; ○: full-scale engine test data ($\frac{1}{3}$-oct bandwidth) measured at 115° from duct inlet.

on the geometric duct length. Attenuation spectra for other than the maximum attenuation angle must be incorporated with the directional characteristics of the sound attenuation. Comparisons of attenuation spectra for three different power settings are shown in Figs. 16, 17, and 18 for approach, cutback, and takeoff conditions. Target frequencies are 1750, 2130, and 3100 Hz, for approach, cutback and takeoff conditions, respectively. Theoretical predictions of the sound attenuation for three power settings of a 747/JT9D engine fan exhaust duct are in good agreement with the test data.

During the comparison of theoretical results and full-scale test data, the composite engine noise spectrum was categorized into many components: fan exhaust, turbine exhaust, inlet, jet noise, and noise from other sources. It was assured that, on the basis of noise decomposition, a noise floor was not present over the frequency range requiring maximum attenuation.

IV. CONCLUSION

A study has been made of the sound attenuation based on a solution of the wave equation for a rectangular duct with two sides lined in the presence of a mean flow. A duct with equal linings on two opposite sides is considered. On the basis of the present study, the following conclusions are drawn:

- The fundamental mode (0 mode) in a lined duct is not necessarily the least attenuated mode. Therefore, any study for the sound propagation in a soft-walled duct (finite impedance) based on the fundamental mode alone may lead to an erroneous conclusion (see Fig. 4).

- An analysis of the sound attenuation in a lined rectangular duct has been applied to the case of a lined annular duct. The results of the present investigation confirm the applicability of this analysis to the sound attenuation for the exhaust conditions of aircraft engine operation, provided that the actual treated area and the realistic impedance model are used (see Figs. 16–18).

- The theoretically predicted attenuation spectra are in very good agreement with the test data (both flow duct and 747/JT9D engine at the angle of maximum attenuation) for the exhaust conditions at typical aircraft turbofan engine power settings. For the inlet conditions, comparison of the theoretical and experimental results with no shear shows a poor agreement in the lower frequency ranges.

- Parametric studies conducted in the present investigation have verified important concepts for acoustic lining design. The level of peak attenuation and the tuning frequency of sound attenuation are, for a given duct geometry and flow condition, controlled by the nondimensional flow resistance and the lining depth, respectively. For a given lining configuration, the sound-attenuation spectrum depends on the duct length-to-height ratio. In all cases, the level of peak attenuation and tuning frequency are affected by the Mach number. Figures 5–10 show the effects of physical parameters for lined ducts. A more rigorous parametric study requires the optimization of acoustic lining parameters. This work is being investigated by the author.

ACKNOWLEDGMENTS

The author expresses his appreciation to Dr. F. W. Fischer and Dr. C. G. Hodge III for useful discussions and suggestions during the period of this work. He is also grateful to the 747/JT9D Engine Noise Technology staffs for their supply of the JT9D engine test data and to the Boeing Company for permission to publish this work.

[1] P. M. Morse, "The Transmission of Sound Inside Pipes," J. Acoust. Soc. Amer. **11**, 205 (1939).

[2] L. Cremer, "Theorie der Luftschall-Dämpfung im Rechteckkanal mit Schluckender Want und das sich dabei Ergebende Hochste Dämpfungsmass," Acustica **3**, 249 (1953).

[3] F. W. Fischer and A. O. Andersson, "Optimization of Duct Linings for Sound Attenuation," Boeing Co. Rep. D6-29356TN (1968).

[4] E. J. Rice, "Attenuation of Sound in Soft Walled Circular Ducts," NASA TM X-52442 (1968).

[5] U. Kurze, "Sound Attenuation in a Duct of Periodic Structure," Acustica **21**, 74 (1969).

[6] P. E. Doak and P. G. Vaidya, "Attenuation of Plane and Higher Order Mode Sound Propagation in Lined Ducts," J. Sound Vibration **12**, 201 (1970).

[7] M. J. Benzakein, R. E. Kraft, and E. B. Smith, "Sound Attenuation in Acoustically Treated Turbomachinery Ducts," ASME 69-WA/GT-11 (1969).

[8] E. Meyer, F. Mechel, and G. Kurtze, "Experiments on the Influence of Flow on Sound Attenuation in Absorbing Duct," J. Acoust. Soc. Amer. **30**, 165 (1958).

[9] F. Mechel, P. Mertens, and W. Schilz, "Research on Sound Propagation in Sound Absorbent Ducts with Superimposed Air Streams," AMRL-TDR-62-14, Aerospace Med. Res. Labs., Wright–Patterson AFB (1962), Vols. I–III.

[10] D. Haley, "Flow Duct Testing of Acoustic Lining," Boeing Co. Rep. D3-8026-1 (1969).

[11] U. Ingard, "Influence of a Fluid Motion Past a Plane Boundary on Sound Reflection, Absorption, and Transmission," J. Acoust. Soc. Amer. **31**, 1035 (1959).

[12] W. Eversman, "Theoretical Prediction of the Influence of Mach Number on the Sound Attenuation in a Flow Duct," Boeing Co. Rep. D3-8002 (1969).

[13] E. J. Rice, "Propagation of Waves in an Acoustically Lined Duct with a Mean Flow," NASA SP-207 (1969), p. 345.

[14] D. C. Pridmore-Brown, "Sound Propagation in a Fluid Flowing through an Attenuating Duct," J. Fluid Mech. **4**, 393 (1958).

[15] D. H. Tack and F. F. Lambert, "Influence of Shear Flow on Sound Attenuation in Lined Ducts," J. Acoust. Soc. Amer. **38**, 655 (1965).

[16] P. Mungur and J. M. L. Gladwell, "Acoustic Wave Propagation in a Sheared Fluid Contained in a Duct," J. Sound Vibration **9**, 28 (1969).

[17] P. Mungur and H. E. Plumblee, "Propagation and Attenuation of Sound in a Soft Walled Annular Duct Containing a Sheared Flow," NASA SP-207 (1969), p. 307.

[18] U. J. Kurze and C. H. Allen, "The Influence of Flow and High Sound Pressure Levels on the Attenuation in a Lined Duct," BBN Progress Rep. No. 4 (1969).

[19] S. Mariano, "Effect of a Wall Shear Layer on the Sound Attenuation in Acoustically Lined Rectangular Ducts," J. Sound Vibration 19, 2 (1971).

[20] J. W. Miles, "On the Disturbed Motion of a Plane Vortex Sheet," J. Fluid Mech. 4, 538 (1958).

[21] M. Lessen, J. A. Fox, and H. M. Zien, "The Instability of Inviscid Jets and Wakes in Compressible Fluid," J. Fluid Mech. 21, 129 (1965).

[22] D. I. Blokhintsev, "Acoustics of Nonhomogeneous Moving Medium," NACA TM-1399 (1956).

[23] W. Eversman, "The Propagation of Acoustic Energy in a Flow Duct," Boeing Co. Rep. D3-8152 (1970).

[24] S.-H. Ko, "Acoustic Wave Attenuation in Lined Rectangular Ducts with Uniform Flow and Shear Flow," Boeing Co. Rep. D6-25485 (1971).

[25] J. Atvars and R. A. Mangiarotty, "Parametric Studies of the Acoustic Behavior of Duct-Lining Materials," Proc. Symp. Acoustical Duct Treatments for Aircraft, Philadelphia, Pa. (8 Apr. 1969).